Available online at www.sciencedirect.com
ScienceDirect
Journal of Nuclear Materials 376 (2008) 108–113
journal of nuclear materials
www.elsevier.com/locate/jnucmat

Transformation of Al_2O_3 to $LiAlO_2$ in Pb–17Li at 800 °C

B.A. Pint *, K.L. More

Materials Science and Technology Division, Oak Ridge National Laboratory, Oak Ridge, TN 37831-6156, USA

Received 18 September 2007; accepted 27 December 2007

Abstract

A FeCrAl substrate was pre-oxidized for 2 h at 1000 °C to thermally grow an external Al_2O_3 scale and then isothermally exposed to Pb–17 at.% Li for 1000 h at 800 °C to determine if this layer would protect the underlying alloy from dissolution. After exposure, a small mass gain was measured, indicating that the layer did inhibit dissolution. However, characterization of the external layer determined that it had transformed to $LiAlO_2$ with an increased thickness and a much larger grain size than the original layer. This observation has implications for the use of Al_2O_3 as a permeation barrier in Pb–Li cooled fusion blanket systems.
Published by Elsevier B.V.

1. Introduction

As fusion first wall blanket concepts are down-selected for further development, such as test blanket modules for ITER, the interest in eutectic Pb–Li as a coolant and tritium breeding material has increased [1,2]. One advantage of Pb–Li is that a wider range of materials are compatible with it compared to Li (a disadvantage of Pb–Li is that the solubilities of Fe, Cr and particularly Ni are much higher, resulting in greater dissolution than in liquid Li [3,4]). Because Li dissolves most oxides [5,6], the traditional strategy of protecting high temperature alloys by the formation of a surface oxide is not effective. However, for eutectic Pb–Li, the activity of Li is very low [7] and this allows Al_2O_3 to be considered as a protective layer in this system [8]. Both Al-containing coatings and alloys have been shown to inhibit metal dissolution in Pb–Li [9–14], presumably due to the formation of an external, protective Al-rich oxide layer, such as Al_2O_3. In addition to a corrosion barrier, alumina also has been considered an excellent candidate as a tritium permeation barrier [11,15–17].

Recent work has focused on assessing compatibility issues for conventional alloys with Pb–Li at 700–800 °C [12–14], much higher temperatures than prior investigations in order to explore the upper temperature limit of protective coatings. Promising reductions in the amount of dissolution have been observed in isothermal capsule experiments for model Al-containing Fe- and Ni-base alloys and aluminide coatings on type 316 stainless steel. However, initial characterization of specimens pre-oxidized to form α-Al_2O_3 and then isothermally exposed to Pb–Li at 800 °C showed an abnormally large surface grain size in preliminary characterization [14]. A pre-oxidized specimen of oxide-dispersion strengthened (ODS) FeCrAl was selected for more extensive characterization before and after exposure to Pb–Li for 1000 h at 800 °C. This characterization demonstrated that the initial α-Al_2O_3 layer had transformed to $LiAlO_2$ upon exposure to Pb–Li.

2. Experimental procedure

Specimens of ODS FeCrAl (Plansee alloy PM2000, recrystallized type KK6) with dimensions of ~15 × 18 × 1–1.5 mm and a composition of 67.8Fe–20.0Cr–10.6Al–0.44Ti–0.23Y–0.74O–0.03C–0.02N (all composition are given in at.%) and 50 ppma S were polished to a 0.3 μm finish. Pre-oxidation of both specimens was conducted with a rapid insert to a pre-heated furnace at 1000 °C in dry, flowing O_2 for 2 h. One specimen was then held with Mo wire in a Mo capsule containing 125 g high purity (99.9999%) Pb shot and 0.86 g Li to make Pb–17 at.% Li [14]. The Mo

---

* Corresponding author.
E-mail address: pintba@ornl.gov (B.A. Pint).

0022-3115/$ - see front matter Published by Elsevier B.V.
doi:10.1016/j.jnucmat.2007.12.010

capsule was loaded in an argon-filled glove box and it was then welded shut to prevent interstitial contamination during the test. The Mo capsule was then sealed inside a type 304 stainless steel (SS) capsule to protect it from oxidation. This system was then heated inside a resistively-heated box furnace in air to 800 °C for ∼1 h to allow the Pb and Li to melt. The capsule was then inverted to submerge the specimen in Pb–Li. After 1000 h at 800 °C, the system again was inverted to allow the liquid metal to drain away from the specimen. To remove residual Pb–Li on the specimen, it was soaked in a (1:1:1) mixture of acetic acid, hydrogen peroxide and ethanol [18] for up to 72 h at room temperature.

Specimen mass was measured before and after exposure on a Mettler–Toledo balance with an accuracy of ±0.01 mg/cm^2. The composition of the Pb–Li remaining in the capsule after cooling was determined by inductively-coupled plasma analysis to be Pb–17.3 at.% Li with no Fe, Cr or Al detected (<30–60 ppma detection limit) [14]. Both exposed specimens were characterized using a field emission gun, scanning electron microscope (SEM) equipped with energy dispersive spectroscopy (EDS), X-ray diffraction (XRD) and a Hitachi model HF-2000 transmission electron microscope (TEM) operated at 200 kV as well as a Philips model CM-200 scanning transmission electron microscope (STEM) also operated at 200 kV. Part of the specimen was mounted in epoxy for a metallographic cross-section. Cross-sectional TEM specimens were prepared using focused ion beam (FIB) thinning [19]. A W layer was applied to protect the outer surface of the reaction product from ion beam damage during thinning.

3. Results

The specimen mass gain after pre-oxidation for 2 h at 1000 °C in O_2 was 0.08 mg/cm^2. These conditions were selected to ensure the formation of an exclusive α-Al_2O_3 surface layer. Oxidizing at lower temperatures risks the formation of less protective, faster-growing metastable alumina polymorphs such as θ-Al_2O_3 [20–23]. Assuming fully-dense α-Al_2O_3, this mass gain corresponds to a ∼0.4 μm thick oxide layer. After exposure to Pb–Li for 1000 h at 800 °C, the specimens gained an additional 0.24 mg/cm^2. In contrast to the mass gain for the ODS FeCrAl specimen, an unoxidized specimen of type 316 SS had a mass loss of 17.3 mg/cm^2 after the same 800 °C exposure [14]. After 1000 h at 700 °C, unoxidized ODS FeCrAl lost 0.2 mg/cm^2 while a 316 SS specimen lost 3.8 mg/cm^2 [13].

The initial characterization [14] of the ODS FeCrAl specimen surface after exposure to Pb–Li showed a uniform adherent surface oxide layer with coarse-grains, Fig. 1(b), unlike the fine-grained alumina observed after pre-oxidation, Fig. 1(a). Nodules on the surface of pre-oxidized ODS FeCrAl (arrows in Fig. 1(a)) were typically rich in Y and Ti, but were absent after Pb–Li exposure. In cross-section, the surface layer after Pb–Li exposure was dense and adherent but obviously thicker, Fig. 2, consistent with the mass gain. Oxide nodules formed during pre-oxidation, like those observed in plan-view, Fig. 1(a), could

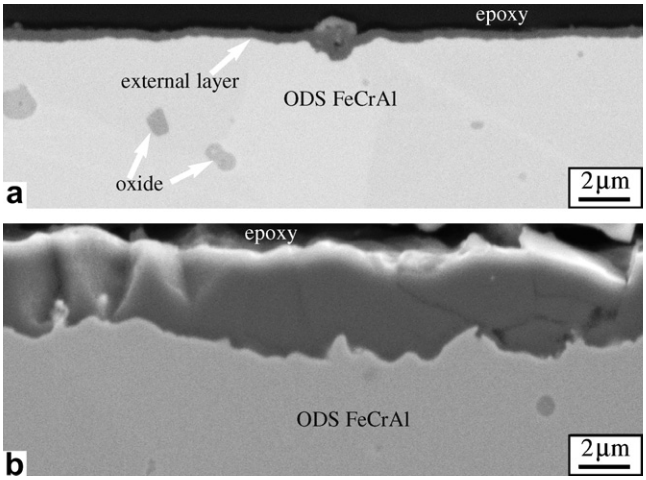

Fig. 2. SEM secondary electron images of polished cross-sections of ODS FeCrAl (a) after pre-oxidation for 2 h at 1000 °C and (b) after pre-oxidation and subsequent exposure for 1000 h at 800 °C in Pb–Li.

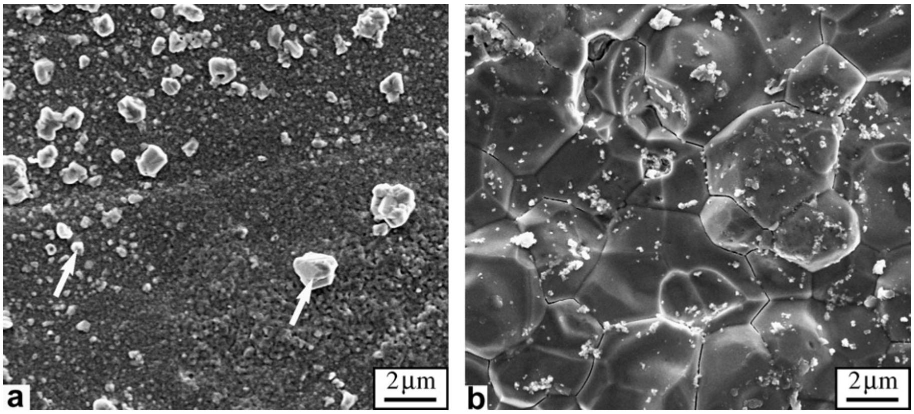

Fig. 1. SEM secondary electron plan-view image of the oxide on ODS FeCrAl (a) after oxidation for 2 h at 1000 °C and (b) after oxidation and exposure to Pb–Li at 800 °C. Arrows in (a) indicated oxide nodules typically rich in Y and/or Ti.

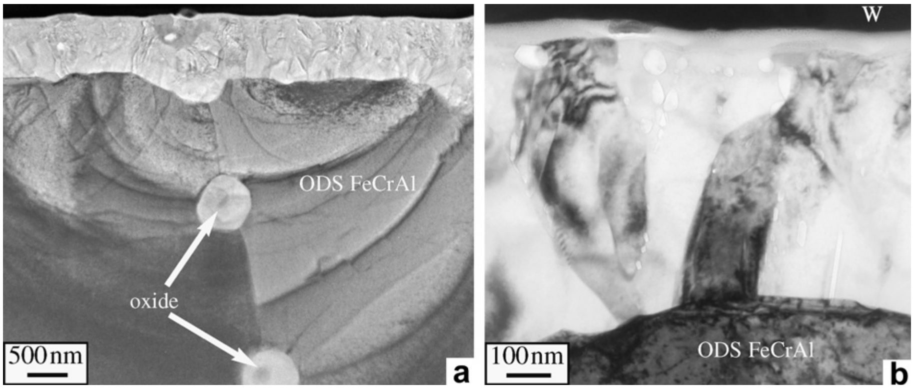

Fig. 3. TEM bright field images of the cross-section of the α-Al_2O_3 scale formed on ODS FeCrAl after 2 h at 1000 °C in dry O_2. The W coating protected the oxide surface during FIB specimen preparation.

be embedded in the surface oxide and cause local variations in the thickness, Fig. 2(a). Coarse, Al-rich oxide particles can be seen in the metal in both cross-sections. The small diameter of these nodules and particles prevented an accurate determination of their composition by SEM/EDS.

Because the pre-oxidized α-Al_2O_3 layer was so thin, TEM from cross-section specimens was necessary to characterize the oxide scale microstructure formed during pre-oxidation, Figs. 3 and 4. After a relatively short exposure of 2 h at 1000 °C, a columnar α-Al_2O_3 grain structure developed with the grains elongated normal to the metal–oxide interface, Fig. 4(a). This is the typical grain structure observed for Y-doped α-Al_2O_3 formed on FeCrAl [23,24]. The outer oxide layer (top ~100 nm) was enriched in Fe and Cr, (arrows in Figs. 4(b) and (c)) which is typical of the initial transient stage of oxidation for a FeCrAl alloy and indicative of an inward growing oxide [25]. However, closer to the metal–oxide interface, the oxide is α-Al_2O_3 containing only minor impurities, Fig. 4. As found in many studies [23,26,27], Y and Ti ions were segregated to the oxide grain boundaries as well as in small oxide precipitates (arrows in Figs. 4(d) and (e)). Fine voids also were observed in the oxide (lighter areas in Fig. 3(b) and darker areas in Fig. 4(a)), but generally the layer was dense and adherent. A faceted metal–oxide interface also was evident.

Consistent with the metallographic cross-section, the TEM cross-section of the oxide layer after Pb–Li exposure was much thicker with much larger grains, Fig. 5. Where grain boundaries intersected the metal-scale interface, the oxide was locally thicker, arrows in Fig. 5(a). The large metal protrusion, arrow in Fig. 5(b), is typical of inward growth along oxide grain boundaries and has been observed in Pt-containing alumina-formers [28,29]. The nucleation of smaller grains at the metal-scale interface is not typical of α-Al_2O_3 formation. However, rapid grain growth and densification were observed when a vapor-deposited Y_2O_3 coating was exposed to Li [30].

Selected area diffraction (by TEM) of the surface layer after exposure was not consistent with the rhombohedral α structure. The lattice spacings measured from diffraction patterns matched closely with the tetragonal structure of

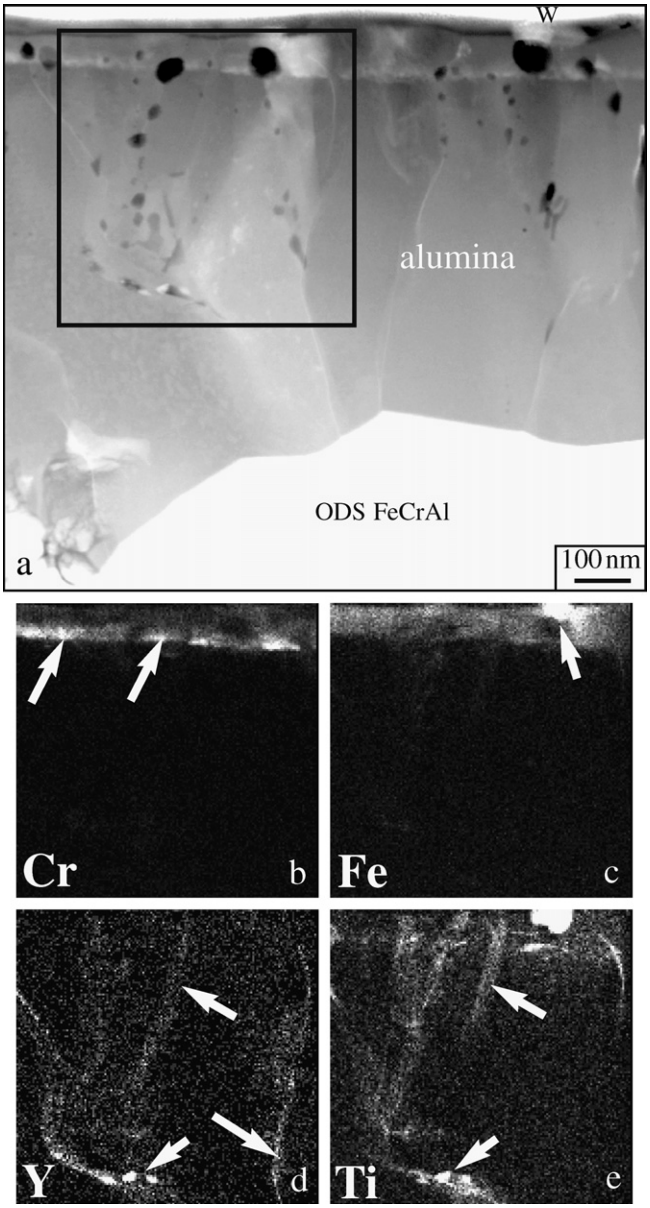

Fig. 4. Cross-section of the α-Al_2O_3 scale formed on ODS FeCrAl after 2 h at 1000 °C in dry O_2, (a) STEM high angle annular dark field image and EDS X-ray maps from the box in (a): (b) Cr, (c) Fe, (d) Y and (e) Ti.

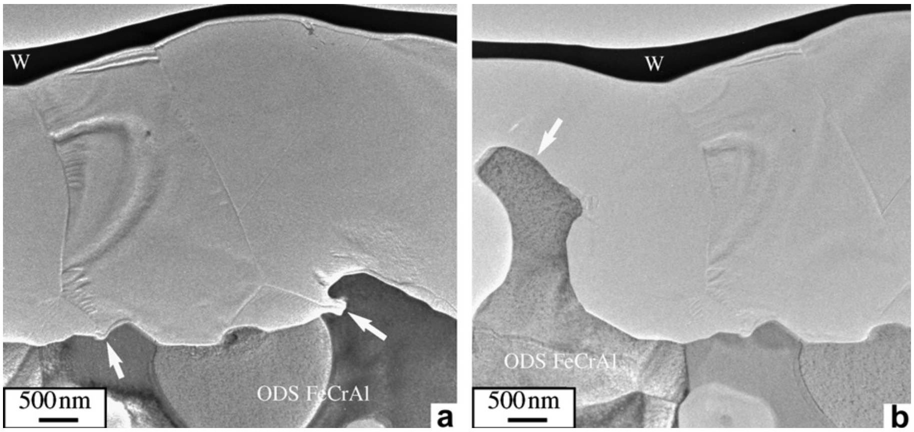

Fig. 5. TEM bright field images of the $LiAlO_2$ layer on the surface of pre-oxidized ODS FeCrAl after exposure to Pb–Li at 800 °C for 1000 h.

$LiAlO_2$. This observation was confirmed using XRD, where all of the major peaks on the Pb–Li exposed specimen were matched with JCPDS card #38-1464 for tetragonal $LiAlO_2$, Fig. 6(b). The XRD spectrum for the unexposed α-Al_2O_3 scale is shown in Fig. 6(a) with peaks matching JCPDS card #83-2080. The peaks are much weaker because of the thinner oxide and the texture of the columnar grains. Typical SEM and TEM chemical analysis using EDS detected Al and O but could not detect Li because of its low atomic number, thus the prior incor-

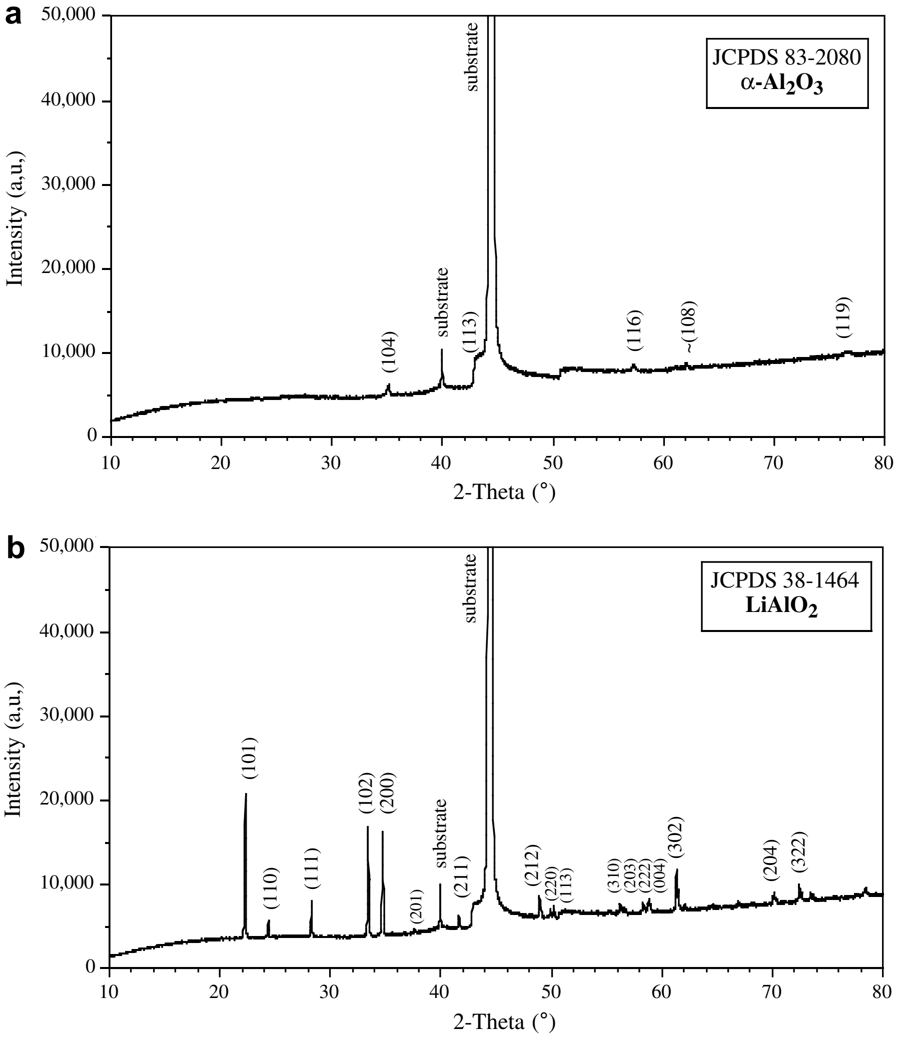

Fig. 6. X-ray diffraction from ODS FeCrAl (a) after pre-oxidation for 2 h at 1000 °C and (b) after pre-oxidation and subsequent exposure for 1000 h at 800 °C in Pb–Li.

rect assumption of Al_2O_3. The $LiAlO_2$ TEM section was easily damaged by the electron beam. Therefore, more extensive chemical analysis (such as Fig. 4 for the α-Al_2O_3 section) was not possible.

4. Discussion

While only a single observation, the transformation of α-Al_2O_3 to $LiAlO_2$ at 800 °C in Pb–Li confirms a hypothesis [16] for the problems that have been observed with using alumina as a permeation barrier in Pb–Li [11,16]. The hydrogen permeation reduction factor dropped from >100X in gas to only 15X when the alumina barrier layer was exposed to Pb–Li [11]. A hydrogen permeability for $LiAlO_2$ was not found in the literature. However, considering the permeability is the product of the solubility and the diffusivity, the tritium diffusivity for $LiAlO_2$ has been estimated to be 2–3 orders of magnitude faster than Al_2O_3 at 500–700 °C [15,31]. Combined with the low tritium solubility in α-Al_2O_3, this difference suggests that the transformation should significantly increase the hydrogen (and tritium) permeation of this layer. However, the $LiAlO_2$ layer seems to perform reasonably well as a corrosion barrier. The observed mass gain can be attributed to reaction of Al_2O_3 with Li to form $LiAlO_2$ and further reaction with O in the Pb–Li (~1300 ppma starting content [14]) to form additional $LiAlO_2$.

The prior thermodynamic analyses did indicate that $LiAlO_2$ was more stable than Al_2O_3 in the presence of Pb–Li [8,16]. However, the kinetics of this transformation require further study as 800 °C is a relatively high temperature for most fusion blanket operating temperatures. At lower temperatures, the transformation could be much slower or negligible. However, the rapid diffusion of Li through most materials suggests that this reaction could occur at temperatures below 800 °C.

One point to emphasize in these results is that the alumina formed on ODS FeCrAl is quite different from the alumina formed on an aluminide coating or by a fabrication process like MOCVD [11]. The presence of Y has long been known to have a dramatic beneficial effect on alumina adhesion to FeCrAl [32]. Yttrium also reduces the oxide microstructure and growth rate and changes the growth mechanism [23,33]. While this particular alloy was selected as a model substrate for evaluation and is no longer commercially available, other commercial alloys with reasonable creep strength are available [34]. The general class of FeCrAl alloys may be sufficiently compatible with Pb–Li to be used without a coating outside of the first wall of a fusion reactor. However, compatibility needs to be further studied in flowing, non-isothermal Pb–Li.

5. Summary

The reaction product on ODS FeCrAl was characterized before and after exposure to Pb–17Li for 1000 h at 800 °C. Pre-oxidation for 2 h at 1000 °C formed an adherent, continuous α-Al_2O_3 layer on the surface. After exposure to Pb–Li, the layer transformed to $LiAlO_2$ with an increase in thickness and grain size. However, the $LiAlO_2$ layer apparently maintained the expected corrosion resistance as alloy dissolution was not observed under isothermal conditions for 1000 h at 800 °C.

Acknowledgments

The research was sponsored by the US Department of Energy (DOE), Office of Fusion Energy Sciences, Fusion Energy Materials Program, under Contract DE-AC05-00OR22725 with UT-Battelle, LLC. D.F. Wilson and J.R. DiStefano consulted on the experimental procedure. J.L. Moser, K.S. Reeves, T. Brummett and D. Coffey assisted with the experimental work. D. Hoelzer and J.R. DiStefano provided comments on the manuscript.

References

[1] P. Noajitra, L. Bühler, U. Fischer, S. Malang, G. Reimann, H. Schnauder, Fus. Eng. Des. 61&62 (2002) 449.
[2] M. Abdou, D. Sze, C. Wong, M. Sawan, A. Ying, N.B. Morley, S. Malang, Fus. Sci. Technol. 47 (2005) 475.
[3] O.K. Chopra, D.L. Smith, P.F. Tortorelli, J.H. DeVan, D.K. Sze, Fus. Technol. 8 (1985) 1956.
[4] P.F. Tortorelli, J. Nucl. Mater. 191–194 (1992) 965.
[5] J.E. Battles, Inter. Rev. Mater. 34 (1989) 1.
[6] R.J. Lauf, J.H. DeVan, J. Electrochem. Soc. 139 (1992) 2087.
[7] P. Hubberstey, J. Nucl. Mater. 247 (1997) 208.
[8] P. Hubberstey, T. Sample, A. Terlain, Fus. Technol. 28 (1995) 1194.
[9] H. Glasbrenner, Z. Peric, H.U. Borgstedt, J. Nucl. Mater. 233–237 (1996) 1378.
[10] H. Glasbrenner, J. Konys, Z. Voss, O. Wedemeyer, J. Nucl. Mater. 307–311 (2002) 1360.
[11] J. Konys, A. Aiello, G. Benamati, L. Giancarli, Fus. Sci. Technol. 47 (2005) 844.
[12] B.A. Pint, J.L. Moser, P.F. Tortorelli, Fus. Eng. Des. 81 (2006) 901.
[13] B.A. Pint, J.L. Moser, P.F. Tortorelli, J. Nucl. Mater. 367–370 (2007) 1150.
[14] B.A. Pint, Fus. Sci. Technol. 52 (2007) 829.
[15] J.D. Fowler, R.A. Causey, D. Chandra, T.S. Elleman, K. Verghese, J. Vac. Sci. Technol. 13 (1976) 401.
[16] T. Sample, A. Perujo, H. Kolbe, B. Mancinelli, J. Nucl. Mater. 283–287 (2000) 1272.
[17] A. Aiello, A. Ciampichetti, G. Benamati, J. Nucl. Mater. 329–333 (2004) 1398.
[18] G. Benamati, C. Fazio, I. Ricapito, J. Nucl. Mater. 307–311 (2002) 1391.
[19] L.A. Gianuzzi, F.A. Stevie, Micron 30 (3) (1999) 197.
[20] P.T. Moseley, K.R. Hyde, B.A. Bellamy, G. Tappin, Corr. Sci. 24 (1984) 547.
[21] G.C. Rybicki, J.L. Smialek, Oxid. Met. 31 (1989) 275.
[22] B.A. Pint, J.R. Martin, L.W. Hobbs, Solid State Ion. 78 (1995) 99.
[23] B.A. Pint, A.J. Garratt-Reed, L.W. Hobbs, Mater. High Temp. 13 (1995) 3.
[24] F.A. Golightly, F.H. Stott, G.C. Wood, Oxid. Met. 10 (1976) 163.
[25] W.J. Quadakkers, A. Elschner, W. Speier, H. Nickel, Appl. Surf. Sci. 52 (1991) 271.
[26] T.A. Ramanarayanan, M. Raghavan, R. Petkovic-Luton, J. Electrochem. Soc. 131 (1984) 923.
[27] K. Przybylski, A.J. Garratt-Reed, B.A. Pint, E.P. Katz, G.J. Yurek, J. Electrochem. Soc. 134 (1987) 3207.

[28] E.J. Felten, F.S. Pettit, Oxid. Met. 10 (1976) 189.
[29] B.A. Pint, J.A. Haynes, K.L. More, I.G. Wright, C. Leyens, in: T.M. Pollack et al. (Eds.), Superalloys 2000, TMS, Warrendale, PA, 2000, p. 629.
[30] B.A. Pint, K.L. More, H.M. Meyer, J.R. DiStefano, Fus. Sci. Technol. 47 (2005) 851.
[31] M. Nishikawa, T. Kinjyo, T. Ishizaka, S. Beloglazov, T. Takeishi, M. Enoeda, T. Tanifuji, J. Nucl. Mater. 335 (2004) 70.
[32] C.S. Wukusick, J.F. Collins, Mater. Res. Stand. 4 (1964) 637.
[33] B.A. Pint, Oxid. Met. 45 (1996) 1.
[34] B. Jönsson, R. Berglund, J. Magnusson, P. Henning, M. Hättestrand, Mater. Sci. Forum 461–464 (2004) 455.